Physiological and Molecular Plant Pathology (1996) 49, 285–306

Flavonoids accumulate in cell walls, middle lamellae and callose-rich papillae during an incompatible interaction between *Xanthomonas campestris* pv. *malvacearum* and cotton

G. H. Dai*, M. Nicole†, C. Andary‡, C. Martinez, E. Bresson, B. Boher, J. F. Daniel and J. P. Geiger
Laboratoire de Phytopathologie, ORSTOM, BP 5045, 34032 Montpellier, France

(*Accepted for publication July 1996*)

Interactions between cotton cotyledons and *Xanthomonas campestris* pv. *malvacearum* were examined. During an incompatible interaction, fluorescence microscopy revealed that flavonoid compounds accumulated within 10 h after inoculation. Electron micrographs showed ultrastructural modifications of cells that exhibited an intense fluorescence suggesting the presence of flavonoids. Phenol-like molecules were produced by cells of infection sites and were found in paramural areas within papillae enriched with callose and in host cell walls and middle lamellae. Histochemistry showed that peroxidase activity and terpenoids were detected in the infected resistant plants, 4 and 48 h after inoculation, respectively. In contrast, no changes in the deposits of lignin, suberin, and catechin were seen in either the infected susceptible or resistant lines. We suggest that early flavonoid accumulation is associated with the hypersensitive reaction of cotton cotyledons to *X. campestris* pv. *malvacearum*. The activity of wall-bound peroxidases may play a role in the incorporation of flavonoids in cell walls and paramural papillae.

INTRODUCTION

Bacterial blight caused by *Xanthomonas campestris* pv. *malvacearum* (Smith) Dye (*Xcm*) is a widespread and destructive disease of cotton (*Gossypium* spp.) in almost every country in the world where this plant grows. Yield losses from severe infection can reach 70% during epidemics in Africa. Angular leaf spot, blackarm and bacterial boll rot are names given to the various stages in the syndrome [*31*]. Considerable variation in resistance to blight occurs in the genus *Gossypium* [*8*], but the highest degree of

* Permanent address: Laboratory of Plant Stress Physiology, Hebei, Academy of Agricultural and Forestry Science, 050051 Shijia-zhuang, Hebei, China.
‡ Laboratoire de Botanique et Phytochimie, Faculté de Pharmacie, Université de Montpellier I, 15 Avenue de C. Flahault 34060 Montpellier, France.
† To whom correspondence should be addressed.
e-mail: nicole@orstom.orstom.fr
Abbreviations used in text: AT, aminotriazole; DHC, 2,7-dihydroxycadalene; HMC, 2-hydroxy-7-methoxycadalene; HR, hypersensitive reaction; LC, lacinilene C; LCME, laciniline C 7-methylether *Xcm*, *Xanthomonas campestris* pv. *malvacearum*.

0885–5765/96/110285+22 $25.00/0

resistance is found in *G. hirsutum* var. *punctatum*. In addition, many Upland varieties exhibit some levels of field resistance or tolerance. Interactions between cotton and *Xcm* are governed by a gene-for-gene relationship [*16*] and several major genes conferring resistance to *Xcm* have been identified in *Gossypium* species. At least 22 major, so-called B-genes, have been reported as dominant factors in *G. hirsutum* [*31*]. The resistant line Reba B50 has two major resistance genes B2, B3 to *Xcm* race 18 while the line Acala 44 is susceptible to this pathogen [*1*, *23*].

The hypersensitive reaction (HR) constitutes one of the most effective responses by which plants defend themselves against attacks by pathogens [*26*]. Studies on the nature of resistance in cotton to bacterial blight have focused on the synthesis of sesquiterpenoids, the main antimicrobial metabolites in cotton. Phytoalexins that inhibit growth of *Xcm* were isolated from inoculated leaves or cotyledons during the HR of resistant lines and identified as 2,7-dihydroxycadalene (DHC), its oxidation product lacinilene C (LC), and lacinilene C 7-methylether (LCME) [*19*, *22*]. The methyl ether of DHC, 2-hydroxy-7-methoxycadalene (HMC), was also found, but at its limit of solubility in water it is not inhibitory to the growth of bacteria [*19*, *49*]. These phytoalexins accumulated in fluorescent hypersensitively necrotic cells adjacent to *Xcm* colonies to concentrations sufficient to account for bacteriostasis [*20*, *21*]. However, not all of the yellow-green fluorescent material in the necrotic areas was extractable suggesting that hypersensitively responding cells also accumulate covalently bound yellow-green fluorescent monomers and polymers [*18*, *21*].

In the present study, we report the occurrence and role of phenolics in interactions of cotton lines from *G. hirsutum* with *Xcm* race 18. Particular attention was paid to the histochemistry of phenolic compounds in infected cotyledons and the associated ultrastructure of phenol-producing cells. Histochemistry of terpenoids and peroxidase activity was also investigated. Our data show that flavonoids accumulated during the incompatible interaction in the infected race-specific resistant line Reba B50, whereas they did not accumulate in the susceptible line Acala 44. Ultrastructural immunocytochemistry indicated that these compounds were associated with callose-rich paramural depositions and the middle lamella.

MATERIAL AND METHODS

Plant Material

Upland cotton (*G. hirsutum* L.) lines used were Acala 44, which is susceptible to all races of *Xcm*, and Reba B50, which is resistant to all known races of *Xcm*, except race 20. Plants were grown under natural light in a greenhouse with the temperature maintained at 30 ± 2 °C and relative humidity at 80 %. Cotyledons were inoculated 11 days after planting.

Bacterial culture, inoculation and sampling

Xcm race 18 was maintained and cultured on LPG agar medium (yeast extract 5 g, peptone 5 g, glucose 5 g, agar 15 g, 1 l distilled water) at 30 °C. For inoculation, bacterial colonies were transferred into LPG liquid medium and gently stirred

overnight at 30 °C. Actively growing cultures were recovered by centrifugation then washed and diluted with sterile distilled water. The inoculum used in these experiments was of 5×10^6 to 10^7 CFU ml^{-1} [*21*]. The abaxial surfaces of cotyledons were infiltrated with inoculum delivered from a needleless syringe until the entire intercellular space was filled. Control cotyledons were infiltrated with sterile water. Following infiltration, untreated, water-infiltrated and inoculated cotyledons were excised 0, 2, 4, 5, 6, 9, 10, 15, 24, 48 h after inoculation. For each histochemical test, four infected plants were examined and at least five sections per cotyledon were investigated. For ultrastructural observations, two infected plants were examined. Two embedded fragments per infiltrated sites—inoculated and water-infiltrated—were sectioned and at least 10 sections were examined per block.

Bacterial growth determination

The time course of bacterial growth was determined by triturating infected or untreated cotyledons in sterile deionized water. After different dilutions, bacterial concentrations were determined by plate counts. Estimation was performed at 0, 2, 6, 24, 48, 72, 96, 120, 168, and 216 h after inoculation, based on three replicates per infected line and per sample.

Histochemistry

Autofluorescence of excised cotyledons was observed under u.v. light (365 nm, 15 w) in a u.v. chamber (CN-15LC, Bioblock Scientific, France). Sections (60–80 μm thickness) cotyledons were cut with a cryostat microtome (Frigocut 2800E, Leica) operating at −20 °C. After staining with the different reagents, the sections were mounted in the reagents or in glycerine/water (15:85 v/v) and examined using a light microscope (Nikon Optiphot) with two filter sets: a u.v. filter set with 365 nm excitation and a 400 nm barrier filter, and a blue filter set with 420 nm excitation and a 515–560 nm band pass filter [*12*, *14*].

Flavonoid compounds were detected using 2-amino-ethyldiphenyl-borinate (Fluka) (Neu's reagent) [*13*, *45*]. Sections were immersed in the reagent for 1–2 min and then mounted in glycerine-water, and observed by epi-fluorescence using a u.v. filter (365 nm) or a blue filter (420 nm). When illuminated with u.v. flavonoids appeared yellow, while they displayed a bright lemon yellow fluorescence when illuminated with blue light. When a yellow-orange fluorescence was observed with blue illumination, phenols were identified as flavanone compounds.

Flavonoid compounds were also detected using Wilson's reagent. Sections were immersed for 15 min in citric acid:boric (Prolabo) (5:5 w/w) in 100 ml absolute ethanol, mounted in glycerine-water and examined by epi-fluorescence [*30*]. Yellow fluorescence indicated the presence of flavonoids.

Vanillin-HCl reagent and 4-dimethylaminocinnamaldehyde (4-DMAC) (Merck) reagent were used to locate catechins and condensed tannins [*25*, *29*]. Stained sections were observed with the light microscope. The red colour indicates the presence of condensed tannins. A saturated solution of $SbCl_3$ in 60 % $HClO_4$ was used to localize the aldehydic sesquiterpenoids in cotyledons [*41*], that stained red when observed with

the light microscope. Two assays for lignin were employed: phloroglucinol-HCl [*24*] and Mirande reagent [*12*, *17*]. Suberin was located using Sudan IV [*37*].

The viability of cells was tested by immersing sections of unfrozen cotyledons in Evans' blue (0·5 % w/v) [*54*] for 15 min, after which they were rinsed with distilled water. Sections were mounted in distilled water and observed microscopically. Dead or damaged cells are unable to exclude Evan's blue and thus became stained deep blue.

Peroxidase (EC 1.11.1.1.7) activity in fresh sections was localized using 3,3′,5,5′-tetramethylbenzidine (TMB, Sigma) [*35*] and guaiacol [*42*] as enzyme substrates. The guaiacol assay was carried out as follows. Tissue sections were collected in distilled water and immersed for 5 min in a medium consisting of 0·2 ml guaiacol (w/v) (Sigma), 100 ml citrate phosphate buffer (pH 6), 0·1 ml hydrogen peroxide 30 % and 1 ml of 0·25 % (v/v) 3 amino-ethyl-carbazole in dimethyl formamide. The sections were rinsed in distilled water, mounted in glycerine-water and observed with the light microscope. Control sections were collected in 0·05 M aminotriazole (AT) in distilled water and immersed in the same medium containing 0·05 M AT, in order to inhibit catalase if present; if this last treatment failed to reduce staining, peroxidase is assumed to be involved.

Light microscopy

Semi-thin sections (1–2 μm) of embedded fragments of plant material prepared for electron microscopy (EM) were observed under the light microscope (Leitz, Diaplan) after staining with toluidine blue 1 % in borax (w/v) pH 8·9.

Electron microscopy

Twenty-two hours after inoculation, areas of infiltrated cotyledons, including (a) the margin of the infected tissues and (b) portions of the non-infected tissues close to the infiltrated area, as well as leaf portions of controls and of untreated cotyledons, were fixed for 2 h in 2·5 % glutaraldehyde (v/v) in 0·1 M cacodylate buffer pH 7·2, rinsed in the same buffer and postfixed for 1 h in 1 % osmium tetroxide in water (w/v). After dehydration in alcohol followed by propylene oxide, samples were embedded in Epon (TAAB, England). Impregnation of cotyledon fragments in resin and resin polymerization were performed according to the company's recommendations. After sectioning, semi-thin sections (1–2 μm) were stained with toluidine blue and examined with a light microscope. Thin sections (80–90 nm) were stained with 4 % uranyl acetate in distilled water and lead citrate, before being examined under a Jeol 100EX electron microscope operating at 80 kv (Laboratoire de Phytovirologie des Régions Chaudes, CIRAD).

Localization of phenol-like compounds using gold-complexed laccase

Localization of phenols was performed with a purified laccase (EC 1.10.3.2) conjugated to colloidal gold [*3*]. Purified protein (70 μg) was added to stabilize 10 ml of the gold solution at pH 5·02. The sections were labelled for 30 min at 25 °C on a drop of the gold-probe (pH 6·0). Specificity of labelling was assessed by incubating sections

with the gold-complexed laccase previously incubated with guaiacol 1 % (v/v), ferrulic acid 0·25 M or chlorogenic acid 0·15 M.

Localization of β-1,4-glucans using gold-complexed exoglucanase

β-1,4-glucans were localized using a purified exoglucanase complexed to gold at pH 9 [*4*]. Sections were labelled for 30 min at 25 °C on a drop of the probe (pH 6·5), before rinsing and staining. Specificity of labelling was assessed by incubating sections with the gold-complexed protein saturated with an excess of β-1,4-glucans from barley.

Immunocytochemistry

Polyclonal antibodies raised against β-1,3-glucans (CRB, U.K.) were used to locate callose [*46*]. Sections from epon-embedded cotyledons were incubated for 30 min at 25 °C on a drop of primary antibodies (1/2000 in 0·1 M PBS pH 7·2—1 % BSA—0·05 % Tween) before being incubated on gold-labelled goat anti-rabbit antibodies (1/20) (GAR-15, Biocell, U.K.).

Monoclonal antibody JIM5 raised against un-esterified epitopes of pectin were used to visualize galacturonic acid-containing molecules. Immunogold localization of pectin was performed as described by Knox *et al.* [*38*]. Sections from epon-embedded cotyledons were incubated on a drop of primary antibodies for 2 h at 37 °C and then on a drop of gold-labelled goat anti-rat antibodies (GAT-10, Biocell, U.K.) for 30 min at 37 °C.

Specificity of labelling was assessed through the following control experiments performed on sections from untreated and infected cotyledons; (i) incubation with the antiserum previously adsorbed with the antigen, laminarin and galacturonic acids respectively; (ii) incubation with pre-immune rabbit or rat serum instead of the primary antiserum; and (iii) omission of the primary antibody incubation step.

RESULTS

Symptoms

In the resistant line, Reba B50, modifications of infected tissues were visible 6 h after infection at sites where the inoculum was infiltrated, as compared to cotyledons that were infiltrated with water. Ten to twenty-four hours (Fig. 1A) after inoculation, light microscopy revealed degraded cells in the infected portion of cotyledons (Fig. 1B) while tissues adjacent to the necrosis showed no apparent modifications. The cytoplasm of cells in the necrotic area but close to the non-infiltrated zone (Fig. 1C) stained intensely with toluidine blue. Seventy-two hours after infiltration, the necrotic areas of infected cotyledons became dry while the healthy portions did not. Infiltration of the resistant cotyledons with sterile water did not induce the formation of necrotic areas (Fig. 2A). In the susceptible line, Acala 44, rapid degradation of the infected tissues did not occur (Fig. 2B). Rather, water-soaked lesions developed 5–8 days after infection caused modifications of the tissue as shown by light microscopy.

Histochemistry

Autofluorescence and histochemical reactions are listed in Table 1.

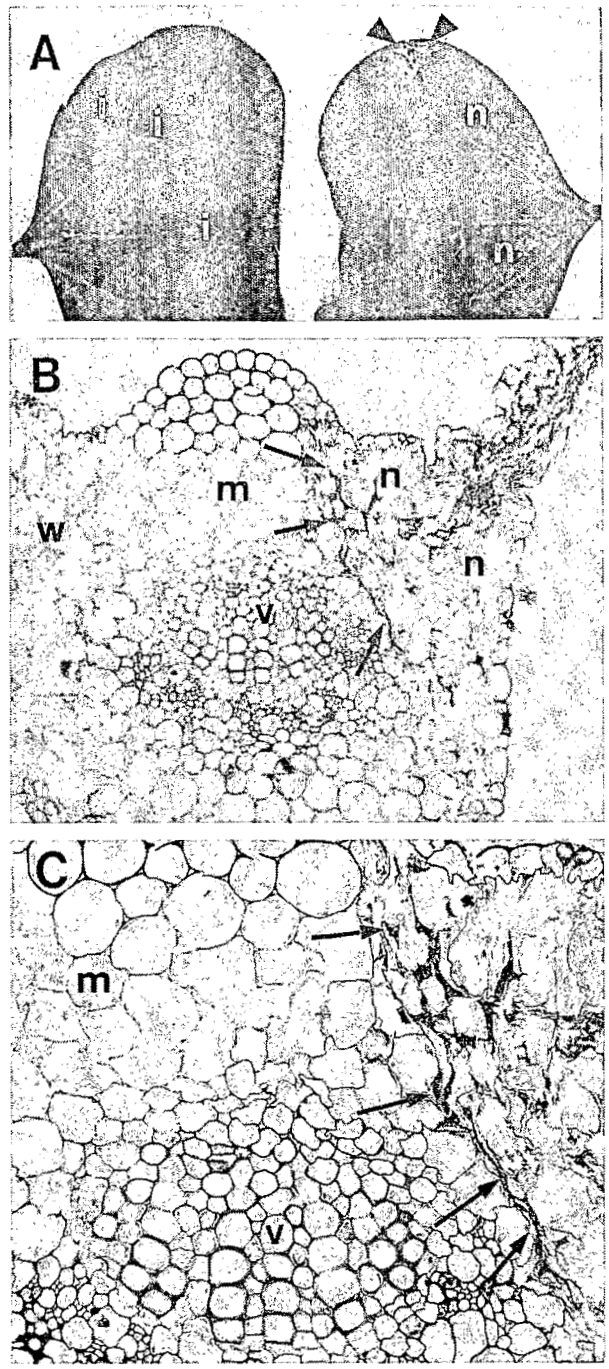

FIG. 1. (A) Cotyledons of the resistant cotton line Reba B50 infiltrated with *Xanthomonas campestris* pv. *malvacearum* (right) or with distilled water (left), examined under u.v. illumination (365 nm). A yellow-green autofluorescence (right) is seen at the margin of the necrotic areas (arrowheads) 22 h after infiltration with the inoculum. Such a fluorescence was not detected in the water-infiltrated cotyledon (left) (i: water-infiltrated area; n: necrotic area) (× 1). (B and C) Semi-thin transverse sections of an infected cotyledon from the resistant cotton line Reba B50, 22 h after inoculation; sections are stained with toluidine blue. In the infected area (n), collapsed host cells and cells located at the margin (arrows) of the necrosis contain a dense cytoplasm. No apparent cell modifications are seen in the vascular tissues (v) and mesophyll cells (m) adjacent to the necrotic are (n). (B: × 200; C: × 500).

Reproduced here at 80%.

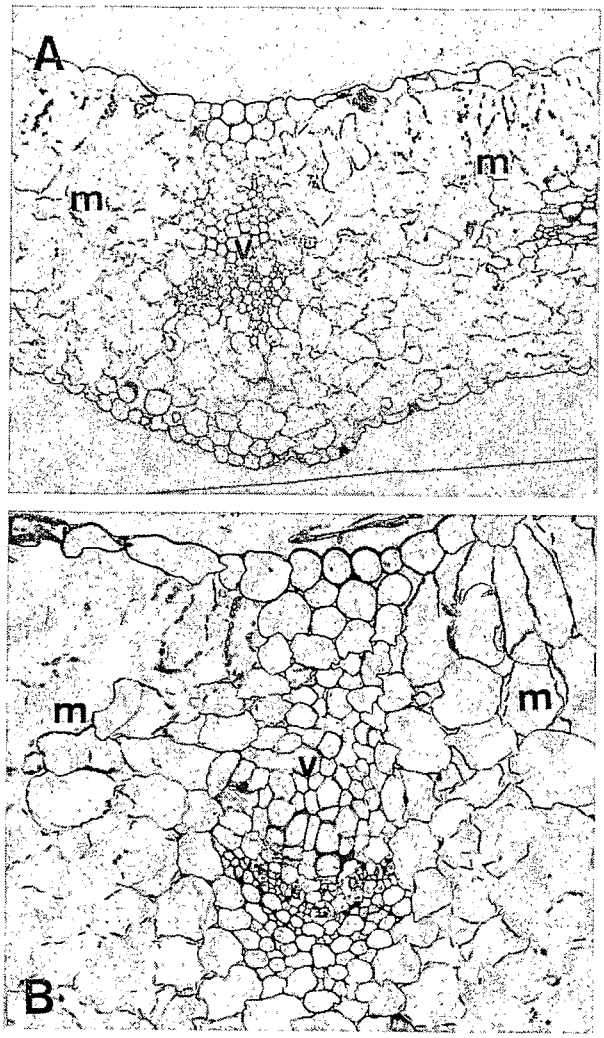

FIG. 2. Semi-thin transverse sections of cotyledons (A) from the resistant cotton cultivar Reba B50, 22 h after infiltration with distilled water and (B) in infected cotyledons from the susceptible line, Acala 44, 22 h after infection. Sections are stained with toluidine blue. Necrotic areas are not seen in the vascular tissues (v) or the mesophyll (m) in either cotyledons (A: ×200; B: ×500). Reproduced here at 80%.

Autofluorescence: In the resistant line, yellow-green autofluorescence was emitted during excitation at 365 nm in the infiltrated areas 2 h after inoculation. The intensity of this autofluorescence increased greatly by 24 h, while a strong yellow-whitish autofluorescence was emitted in cells at the margin of the infiltrated area (Fig. 1A right). Cotyledons infiltrated with sterilized water (Fig. 1A left) and healthy cotyledons (not shown) did not display any fluorescence. In the susceptible line, a weak yellow-green autofluorescence was detected 4 h after infiltration with the inoculum. Nine hours after infection, a weak yellow fluorescence was detected in the lower epidermal and stomatal cells and in cells located at the margin of the degraded area (not shown).

Flavonoid detection: Neither sections from infected cotyledons of the susceptible line (Fig. 3A) nor the uninoculated controls (not shown) exhibited yellow fluorescence following

TABLE 1
Autofluorescence, flavonoid and sesquiterpene accumulation, and peroxidase activity in cotton cotyledons infected with Xanthomonas campestris *pv.* malvacearum.

Reagent	Specificity	Cultivar*	Reaction according to the time course of infection (h) after infiltration†										Site of reaction‡
			0	2	4	5	6	9	10	15	24	48	
Autofluorescence	Phenolics or terpenoid naphthols (yellow-green)	R	−	±	+	+	+	+	+	+	+	+	A
		S	−	−	±	±	±	±	±	±	±	+	A
Neu's	Flavonoids (yellow/orange)§	R	−	−	−	−	−	+	+	+	+	+	B
		S	−	−	−	−	−	−	−	−	−	−	
Wilson's	Flavonoids (yellow)	R	−	−	−	−	−	+	+	+	+	+	B
		S	−	−	−	−	−	−	−	−	−	−	
Antimony chloride	Sesquiterpenoid aldehydes (red)	R	−	−	−	−	−	−	−	−	−	+	C
		S	−	−	−	−	−	−	−	−	−	−	
Guaiacol	Peroxidase (brown)	R	−	−	+	+	+	+	+	+	+	+	D
		S	−	−	−	−	−	−	−	−	−	−	
TMB	Peroxidase (blue)	R	−	−	−	−	+	+	+	+	+	+	E
		S	−	−	−	−	−	−	−	−	−	−	

* R = Reba B50, resistant; S = Acala 44, susceptible.
† − = no response; ± = weak response; + = strong response.
‡ A: yellow-green autofluorescence diffused in the infiltrated zone. At 4 h, a strong fluorescence was seen at the margin of the infiltrated area in the resistant line.
B: yellow fluorescence was observed first in cells at the margin of the necrotic area, and later in cells within the necrosis of the resistant line.
C: terpenoids were detected in the necrotic area of infected cotyledons of the resistant line.
D: peroxidase activity was detected in spongy mesophyll cells at infection sites 4 h after infiltration of resistant cotyledons. After 5 h, it was also seen in palisade mesophyll cells.
E: in spongy mesophyll cells of the resistant cotyledons, peroxidase was also seen in cell walls.
§ Flavonoids appear yellow or yellow bright when illuminated with u.v. (365 nm) or blue light (420 nm), respectively.

treatment with Neu's or Wilson's reagents. Similar treatment of sections of cotyledons of the resistant line revealed that cells at the margin of the infiltrated tissues emitted a strong yellow fluorescence during excitation at 365 nm, 10 h after infiltration with the inoculum (Fig. 3B). When observed under blue light (420 nm), fluorescence was bright lemon yellow (not shown). In contrast, cells present in the infiltrated tissues emitted very weak yellow fluorescence (Fig. 3B). This yellow fluorescence intensified at 24 h and was observed especially within the part of the infiltrated area that became necrotic (Fig. 3C). Observations at a higher magnification showed that the fluorescence was localized in walls and cytoplasm of cells adjacent to the non-infiltrated tissues of cotyledons (Fig. 3D). A weak yellow fluorescence was also observed in walls of xylem cells. The intensity of the yellow fluorescence decreased at 72 h (not reported in Table 1). These results strongly suggested that flavonoid compounds were induced to form following infiltration by *Xcm* in the resistant line, but not in the susceptible line.

Sections of infected resistant cotyledons were also stained with Evan's blue. Ten hours after infiltration with the pathogen, cells in the middle of the infiltrated tissues stained blue. In contrast, flavonoid-containing cells at the margin of the necrotic tissue did not stain blue, indicating that accumulation of flavonoid phenols occurred in the cells present at the margin of the infiltrated areas.

Sesquiterpenoid aldehyde: The red colour of tissues after treatment with $SbCl_3$ revealed the occurrence of aldehydic sesquiterpenoid compounds. After treatment of healthy cotyledon sections of both lines, only glands at the leaf surface were stained red. In infected resistant and susceptible cotyledons, no accumulation of terpenoids was observed during the first 48 h following infection (Table 1). A positive reaction to $SbCl_3$ was seen from 2 days after inoculation in the necrotic area of the resistant line (not shown).

Catechins or condensed tannins: The red and blue colour of tissue sections treated with the vanillin-HCl and the 4-dimethylaminocinnamaldehyde reagents, indicated the occurrence of catechins or condensed tannins. After treatment of untreated cotyledon sections of both lines, leaf hairs showed a red colour, indicating that catechins or condensed tannins exist constitutively in the cotyledons. After infiltration with inoculum, sections of cotyledons of both lines treated with these reagents did not display any significant modification.

Lignin: Except xylem vessels, which reacted strongly to Mirande's reagent and phloroglucinol-HCl, no lignin-like material was evidenced in the infected cotyledon tissues of either line, nor in cells located at the margin of the infiltrated areas that became necrotic (Fig. 3E).

Suberin: Sections of untreated and infected cotyledons of both lines showed no staining with Sudan IV.

Peroxidase activity: In the untreated cotyledons of both lines, epidermal cells and mesophyll cells close to stomata showed a brown colour after staining with guaiacol. Peroxidase activity was detected in the spongy mesophyll cells at the infection sites 4 h after infiltration of resistant cotyledons with inoculum (Table 1). At 5 h, peroxidase activity was also observed in pallisade mesophyll cells. In sections of infected cotyledons from the susceptible line, no reaction with guaiacol was found in mesophyll cells. No staining was observed in sections used for control treatments with AT or without H_2O_2. Peroxidase activity bound to cell walls and located in intercellular spaces, was revealed by TMB in the spongy mesophyll 6 h after infection of cotyledons of the resistant line. This was not observed in the susceptible line (Table 1).

Ultrastructure of infected cotyledons

Ultrastructural observations were made on thin sections from healthy, control and infected cotyledons of both lines, 22 h after inoculation. In the resistant line, phloem cells of veins located close to the necrotic areas displayed various ultrastructural

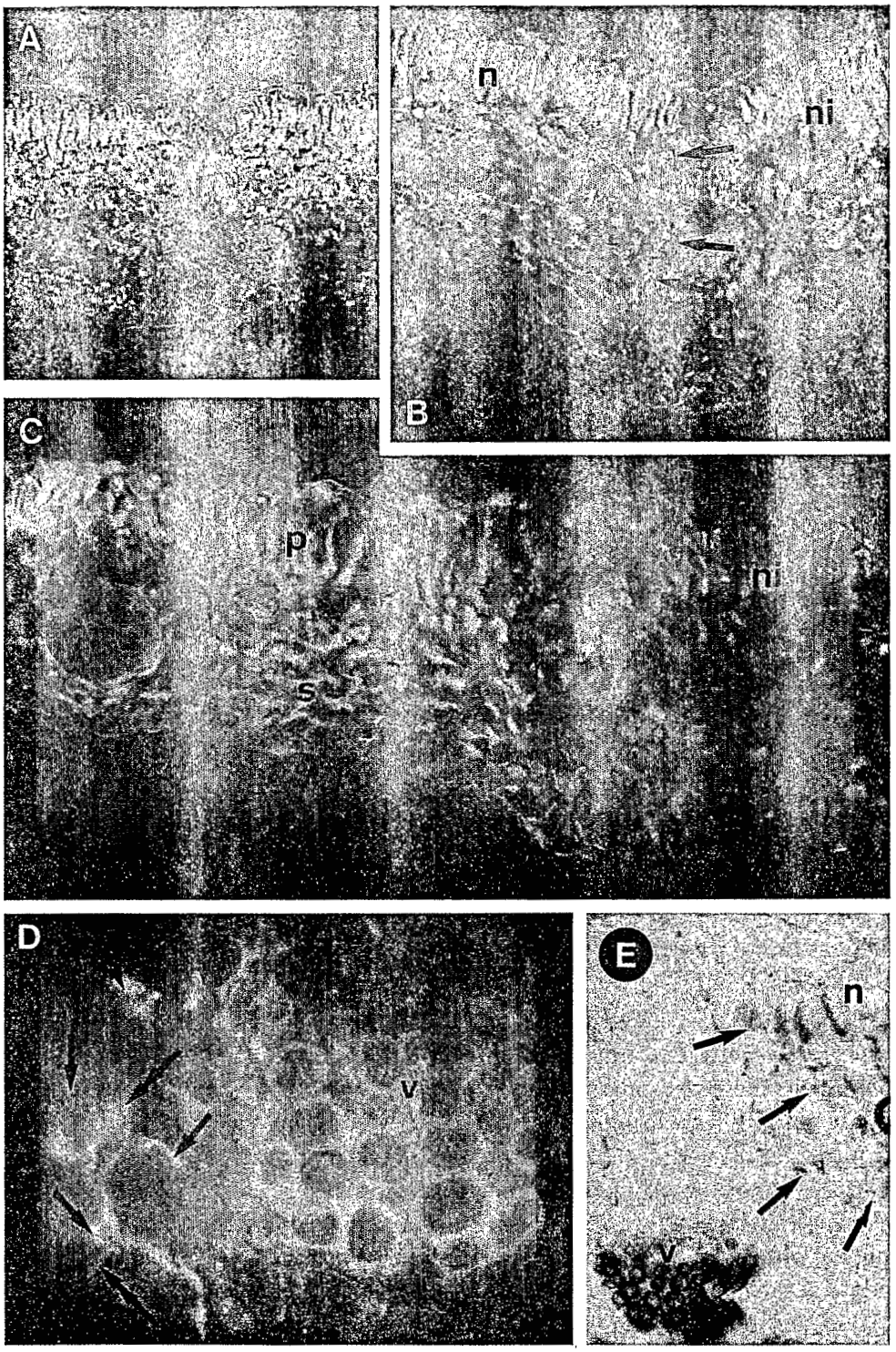

FIG. 3. (A–D) Transverse sections of cotton cotyledons infiltrated with *Xanthomonas campestris* pv. *malvacearum*; sections were treated with the Neu's reagent for flavonoid detection and observed under u.v. illumination. (A) 10 h after infection, no flavonoid accumulation is observed on sections made in cotyledons of the susceptible line Acala 44 as indicated by the absence of a yellow fluorescence (×200). (B) 10 h after infection of the resistant cultivar Reba B50, the yellow fluorescence indicates that flavonoids accumulate at the margin of the necrosis (arrows) while a weak yellow fluorescence only was observed in the infiltrated area (n) at a distance from the margin. Such fluorescence was not detected in the vascular tissues or in the non infected portions of the cotyledon (ni) (×400). (C) 24 h after infection of the resistant cotton cultivar Reba B50,

changes, including cell disorganization (Fig. 4A) or an increase in the electron-density of the cytoplasm (Fig 4A and B). In these cells, the envelopes of chloroplasts (Fig. 4C), the plasma membrane and the endoplasmic reticulum network (Fig. 4D) were highly electron-dense. The infected mesophyll cells at the margin of the necrotic tissues showed a retracted and coagulated cytoplasm in which the structure of organelles was not distinguishable (Fig. 4E). Intensely electron-dense bodies (EDBs) were found in this coagulated cytoplasm and in paramural areas (Fig. 4E). The middle lamella of EDB-containing mesophyll cells was highly electron-dense (Fig. 5A–E). Close contacts between EDBs and the electron-dense middle lamella could be seen when EDBs were located at the margin of the cytoplasm (Fig. 5C) or in intercellular spaces (Fig. 5E). In cells that contained wall appositions, EDBs were found close to, or within them (Fig 5B–D). The pathogen located in intercellular spaces of the necrotic tissues was surrounded by a fibrillar bacterial sheath associated with the electron-dense middle lamella (Fig. 5E). Fragments from this electron-dense middle lamella were enclosed within the bacterial sheath (Fig. 5E) or in close contact with it. Some bacterial cells contained electron-dense particles (Fig. 5E) while others did not (Fig. 6A). Observations of necrotic areas at a distance from the margin revealed that degraded cells contained residual cytoplasmic fragments (Fig. 6B) and few EDBs. In sections from healthy tissues from water-infiltrated cotyledons (Fig. 6C), no EDBs were seen in mesophyll cells; the middle lamella did not display any electron-dense area.

In the infected susceptible line, disorganization of mesophyll cells consisted of a disorganization of organelles, including nuclei (Fig. 6D) and chloroplasts (Fig. 6E). The cytoplasm of cells in the infiltrated areas was not coagulated and no EDBs were detected in the degraded tissues.

Localization of phenol-like compounds

No significant labelling by gold-complexed laccase was observed over host cell structures, including EDBs, cell walls and middle lamella of either infected or healthy tissues.

Localization of β-1,4-glucans

Plant cell walls were evenly labelled after incubation of sections with the β-1,4-exoglucanase conjugated to colloidal gold (Fig. 7A). Few or no gold particles were seen over the paramural material deposited in the necrotic area.

---

a strong yellow fluorescence indicates that flavonoids are localized in the whole infiltrated area both in the spongy (s) and the palisade (p) mesophylls. The tissues adjacent to the infected zone (ni) do not display any specific yellow fluorescence (× 400). (D) 24 h after infection of the resistant cotton cultivar Reba B50, the yellow fluorescence is localized in the cytoplasm (arrows) and the cell walls (double arrows) of mesophyll cells at the margin of the infiltrated area. A weak yellow fluorescence is also visible in the uninfiltrated xylem vessels (v), adjacent to the infected area (× 1600). (E) Transverse section in a cotyledon of the resistant cotton cultivar Reba B50, 48 h after infiltration with *Xanthomonas campestris* pv. *malvacearum*; sections were treated with phloroglucinol-HCl for lignin detection and observed under visible light. The red colour indicates the occurrence of lignin in cell walls of xylem vessels (v). No staining is seen in cells at the margin of the necrotic area (n) and in cells where flavonoids accumulated (arrows) (× 400).

Reproduced here at 80 %.

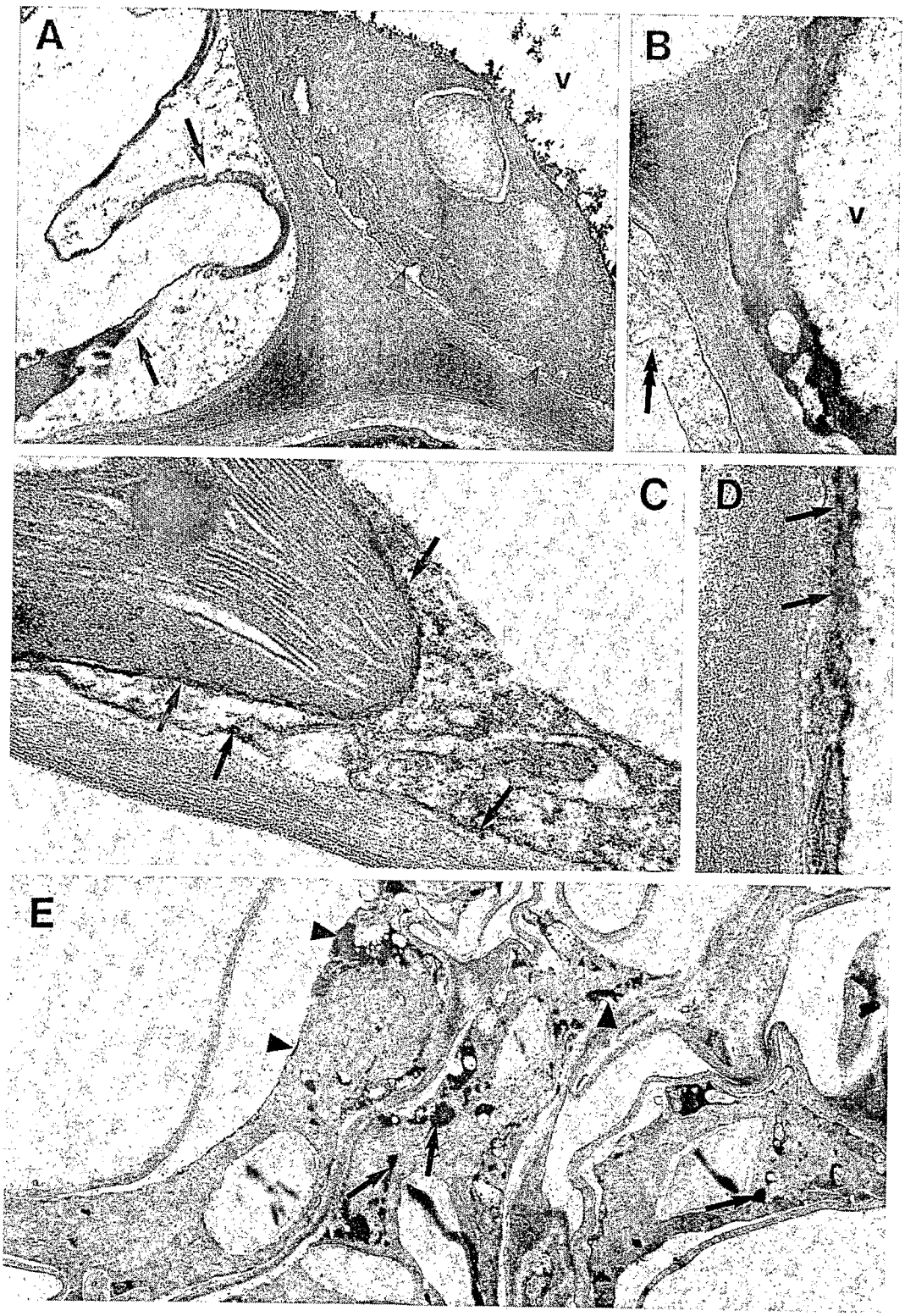

FIG. 4. Transmission electron micrographs of transverse sections of an infected cotyledon from the resistant cotton cultivar Reba B50, 22 h after infiltration with the pathogen. (A and B) Cells located in the phloem close to the margin of the necrotic area display various stages of cell disorganization, including cytoplasm (A, arrows) and membrane (A, arrowheads) retraction. An apparently non degraded cell (B, double arrows) can be seen adjacent to altered cells (ml: middle

Immunolocalization of JIM 5 epitopes
Immunocytolocalization of pectin epitopes after treatment of sections with JIM 5 anti-pectin monoclonal antibody followed by GAT-gold antibodies revealed that labelling occurred over the middle lamellae (Fig. 7B). Few or no gold particles were seen over the paramural material deposited in the necrotic area.

Immunolocalization of β-1,3-glucans
Immunocytolocalization of β-1,3-glucans after treatment of sections with anti-β-1,3-glucans polyclonal antibodies followed by GAR-gold antibodies revealed that labelling occurred over wall appositions in paramural areas of cells located within the necrotic zone (Fig. 7C). Labelled papillae were also seen close to plasmodesmatal areas (Fig. 7D). Callose-containing material mainly occurred at the edge of the infiltrated zone close to the non infected leaf portion rather than in cells located in the middle of the necrosis (not shown). No similar deposits were detected in cells of the healthy leaf portions, although gold particles decorated electron-lucent material that is normally deposited in phloem sieve tubes (Fig. 7E). Pre-incubation of the antibodies with laminarin to assess labelling specificity yielded negative results (data not shown).

Bacterial growth
The number of bacteria increased rapidly in the inoculated cotyledons of the resistant and susceptible lines until approximatively 72 h (Table 2). At this time, bacterial growth in the resistant line Reba B50 decreased until 216 h after inoculation. The rate of increase of the bacterial population in the susceptible line Acala 44 slowed down slightly approximatively 130 h after inoculation.

DISCUSSION

The present study performed on susceptible and resistant cotton lines shows significant differences in reactions following infiltration of cotyledons with *Xcm*. In the resistant line Reba B50, the limited multiplication of the pathogen was in association with the HR, while in the susceptible plants, bacterial continued to grow until seedling death.

Our observations under u.v. light (365 nm) showed that 2 h after infection a yellow-green autofluorescence was more intense in resistant than in susceptible plants. At this time flavonoids and sesquiterpenoid aldehydes, as well as other molecules whose presence was assayed histochemically, did not react with the reagents. This indicates that unidentified compounds were produced at these sites of infection, before necrosis was visible. In resistant lines, terpenoid phytoalexin accumulation occurred during the first 72 h [*27, 49*]. More than 90% of the DHC and more than 75% of the LC and LCME were associated with the fluorescent cells at infection centres [*49*]. Of the fluorescent cells observed in leaf samples 2, 3, and 4 days after inoculation, 98±2%

lamella; v: vacuole) (A and B: ×22000). (C and D) accumulation of electron-dense material is observed in the chloroplast envelope, the plasma membrane (C, arrows) and in the endoplasmic reticulum (D, arrows) (C and D: ×47000). (E) mesophyll cells located at the margin in the infiltrated area (see also Fig. 1C, arrows) contain a coagulated cytoplasm in which membranes, including those of organelles are degraded. Electron-dense bodies occurred in (arrows) and at the periphery of (arrowheads) the coagulated cytoplasm (×9000).
Reproduced here at 80%.

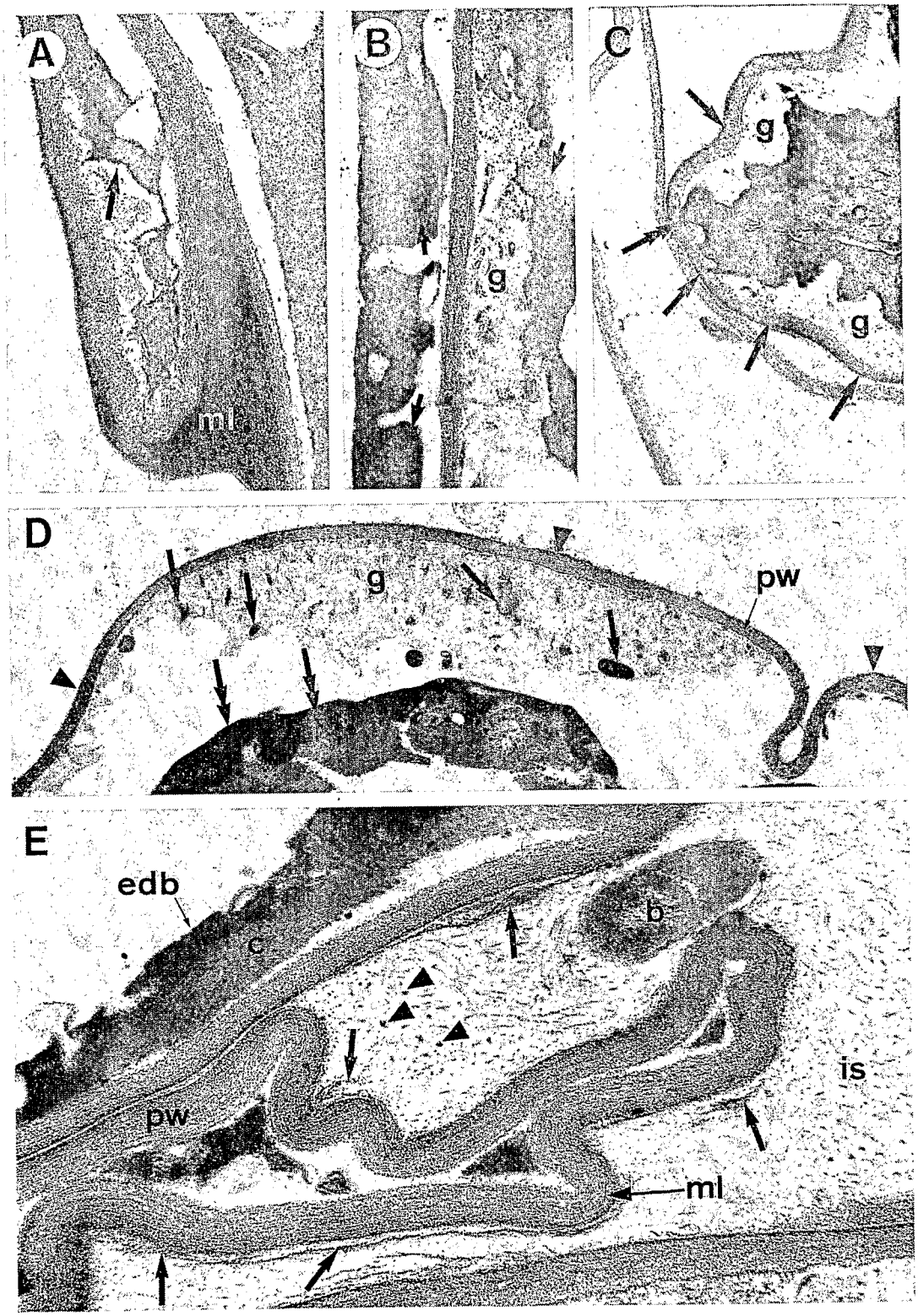

FIG. 5. Transmission electron micrographs of transverse sections in an infected cotyledon from the resistant cotton cultivar Reba B50, 22 h after infiltration with the inoculum. (A) In the mesophyll cell located at the margin of the necrotic area, the middle lamella appears to be highly electron-dense (ml). Note that electron-dense bodies occur in the degraded cytoplasm (arrow) (×30000). (B) Granular-like material (g) is located in the paramural area of a cell at the margin

were dead as indicated by Evans' blue staining. However, not all the yellow-green fluorescent material in the necrotic areas was extracted suggesting that free terpenoid phytoalexins were associated with fluorescent phenolics in necrotic cells [*18*]. In our experiments, it is likely that terpenoids and/or phenolics other than flavonoids were produced at an early stage of infection.

In the infected cotton lines, accumulation of flavonoids in the resistant plants were detected 9 h after inoculation in cells close to the necrotic tissues, while aldehydic sesquiterpenoids were observed later, 48 h after inoculation. Evans' blue staining showed that these flavonoids accumulated in the living cells found at the margin of the necrotic tissues. This indicates that these compounds are probably first synthesized in response to *Xcm* in cells that are not yet infected. Phenol-like molecules were not located by the use of a laccase-gold probe, although this enzyme was successfully used in other plant/pathogen systems [*3*, *11*]. This suggests that flavonoids may be translocated towards the HR cells that became necrotic, as reported for sesquiterpenoid phytoalexins in another cotton resistant line [*27*]. Electron microscope observations revealed severe ultrastructural modifications of cells that exhibited the intense fluorescence indicative of flavonoids. We assume that flavonoids are produced within the cytoplasm as spherical and highly EDBs associated with membrane structures. This is consistent with the fact that flavonoid compounds are synthesized within the cytoplasm [*52*]. They were also seen in the paramural areas, often in newly-formed papillae where they predominantly accumulated in primary cell walls and the middle lamellae. Papillae that only differentiated in the resistant infected plants have already been described as a cotton response to *Xcm* [*44*]. In Reba B50, they were found to contain callose, but not cellulose, unesterified pectin epitopes or phenolics targeted by the laccase-gold conjugate. Callose deposits have already been reported in compatible [*7*, *39*] and incompatible [*5*, *9*] plant-bacteria interactions. In the incompatible cotton-*Xanthomonas* pathosystem, paramural material enriched with callose was seen at the edge of the necrotic area. Such papillae have been suggested by Peng and Kuc [*48*] to contain H_2O_2 generated by the oxidative burst associated with the HR. Production of H_2O_2 in cell walls and middle lamellae was demonstrated in the Reba B50 resistant cotyledons infected by *Xcm* race 18 (unpublished data).

The flavonoids that were detected in the infected resistant host were fixed to polysaccharides including cellulose, pectin and callose. It was not possible to extract them in their native forms with organic solvents, e.g. methanol, acetone or acetonitrile, or with acid or alkaline medium (data not shown). Although such compounds were

in the necrotic area. Electron-dense bodies occur in the degraded cytoplasm (arrows) (×45000). (C) The coagulated cytoplasm (c) of a mesophyll cell located at the margin in the necrotic area is surrounded by electron-dense bodies which are in close contact with the paramural and granular material (g). Association of electron-dense bodies are seen with the primary cell wall (double arrows). Notice that the middle lamella displays electron-dense portions (arrows) (×16000). (D) Electron-dense bodies (double arrows) located in the paramural area of this mesophyll cell are also seen in contact with the paramural papilla (g) (arrows). Note that portions of the middle lamella are electron-dense (arrowheads) (pw: primary cell wall; ×16000). (E) The bacterial cell (b) localized in the intercellular space (is) is surrounded by a fibrillar sheath which is in close contact with the electron-dense middle lamella (ml). Detached fragments from the electron-dense middle lamella (arrows) and dense particles (arrowheads) are seen to occur within the bacterial sheath. Dense granules are also detected in the bacterial cell (c: coagulated cytoplasm; edb: electron-dense granules; pw: primary cell wall) (×46000).

Reproduced here at 80%.

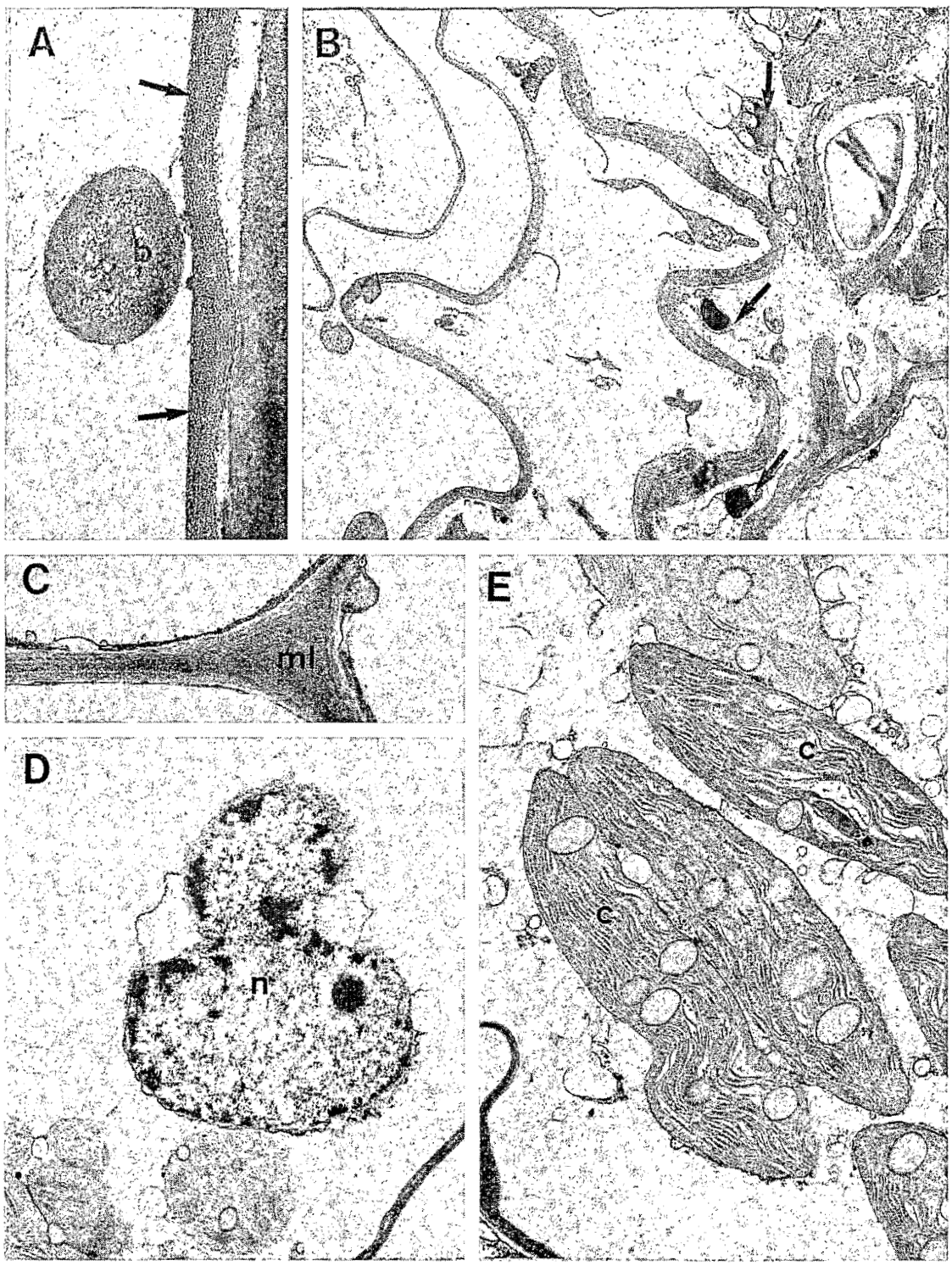

FIG. 6. Transmission electron micrographs of transverse sections in an infected (A, B) or water-infiltrated (C) cotyledon from resistant cotton cultivar Reba B50 and in infected cotyledons from the susceptible cultivar Acala 44 (D, E), 22 h after infiltration with the pathogen. (A) An apparently non degraded bacterial cell (b) is located close to the electron-dense middle lamella (arrows) (c: coagulated cytoplasm; × 22 000). (B) The infected area at a distance from the margin of the necrotic tissue contains cells with advanced patterns of cytoplasmic degradation. Few electron-dense bodies (arrows) are visible in the residual cytoplasm (× 9500). (C) The middle

seen in the remaining cytoplasm of necrotic cells, it is likely that they occurred at such low amounts that they could not be extracted with traditional methods [*14*]. This points out the advantages of cytology that allows more accurate observations of localized accumulation of defence molecules.

In infected cotton cotyledons, the accumulation of flavonoids in the necrotic tissues probably contributes to the limitation of bacterial multiplication. Jalali *et al.* [*36*] reported that anthocyanin compounds, the most conspicuous class of flavonoids [*33*], play a vital role in cotton resistance by inactivating both polygalacturonase and methylesterase activity. Our electron microscope observations revealed that the pathogen was restricted to intercellular spaces within the necrotic area. Degradation of plant cell middle lamellae by xanthomonads [*6*], including *Xcm* [*10*] leads to the accumulation of pectic fragments within the bacterial exopolysaccharide. In infected cotton leaves, those detached portions of middle lamella, that sometimes contained EDBs that we presume to be flavonoid compounds, may be highly toxic for the pathogen whether or not the bacterial cells are in contact with these fragments. Selected flavonoid compounds have been demonstrated to have bactericidal effects against several *Xanthomonas* species [*56*]. But Holliday and Keen [*32*] suggested that the HR occurred even if isoflavonoid accumulation was inhibited. Our data support the hypothesis that flavonoids produced early in infected cotton cotyledons play a role in the defence strategy of cotton. We suggest that they are likely to act before terpenoid phytoalexins since the sesquiterpene cyclase activity, the first enzyme in the biosynthetic pathway of sesquiterpenoid defence compounds, increases only after 20 h post-inoculation [*15*].

Enhancement of peroxidase activity in mesophyll cells 4 h after inoculation of the resistant line suggests that peroxidases could also be involved in cotton defence to *Xcm*. Venere [*55*] demonstrated that the increase in cotton peroxidase activity during the incompatible interaction was accompanied by a decline in the number of bacteria recovered from the inoculated tissue and the accumulation of brown materials in the inoculated site. This author suggested that oxidation of catechin by peroxidase may be a factor in restricting growth of the bacterial pathogen in blight resistant cotton. In *Xanthomonas*-infected rice, one cationic peroxidase has been correlated with the accumulation of lignin-like compounds and a reduction in bacterial multiplication in the leaves at the onset of the HR [*28, 50, 51*]. However, in the present study, modifications in the distribution of catechin and condensed tannins, as well as the occurrence of lignin-like materials, including suberin, were not observed histochemically after inoculation. These results question the role of peroxidase activity in the defence strategy of the plant to *Xcm*.

Although it is known that peroxidases are responsible for membrane oxidative burst during the HR [*26*], a recent study reported that plant peroxidases may also generate antimicrobial phenolics [*40*]. Several phenols, such as flavonols and flavanones, have been reported to be converted into oxidized or polymerized compounds by activated

---

lamella (ml) of cells within the water-infiltrated cotyledons does not display any electron-dense areas; electron-dense bodies are absent in the cytoplasm (× 10000). (D and E) The cytoplasm of these cotyledon mesophyll cells in the susceptible cultivar does not show any electron-dense bodies similar to those occurring in the necrotic areas of the resistant cultivar, although alterations of the cytoplasm are observed (n: nucleus; c: chloroplasts) (C: × 9500; D: × 11500).

Reproduced here at 80%.

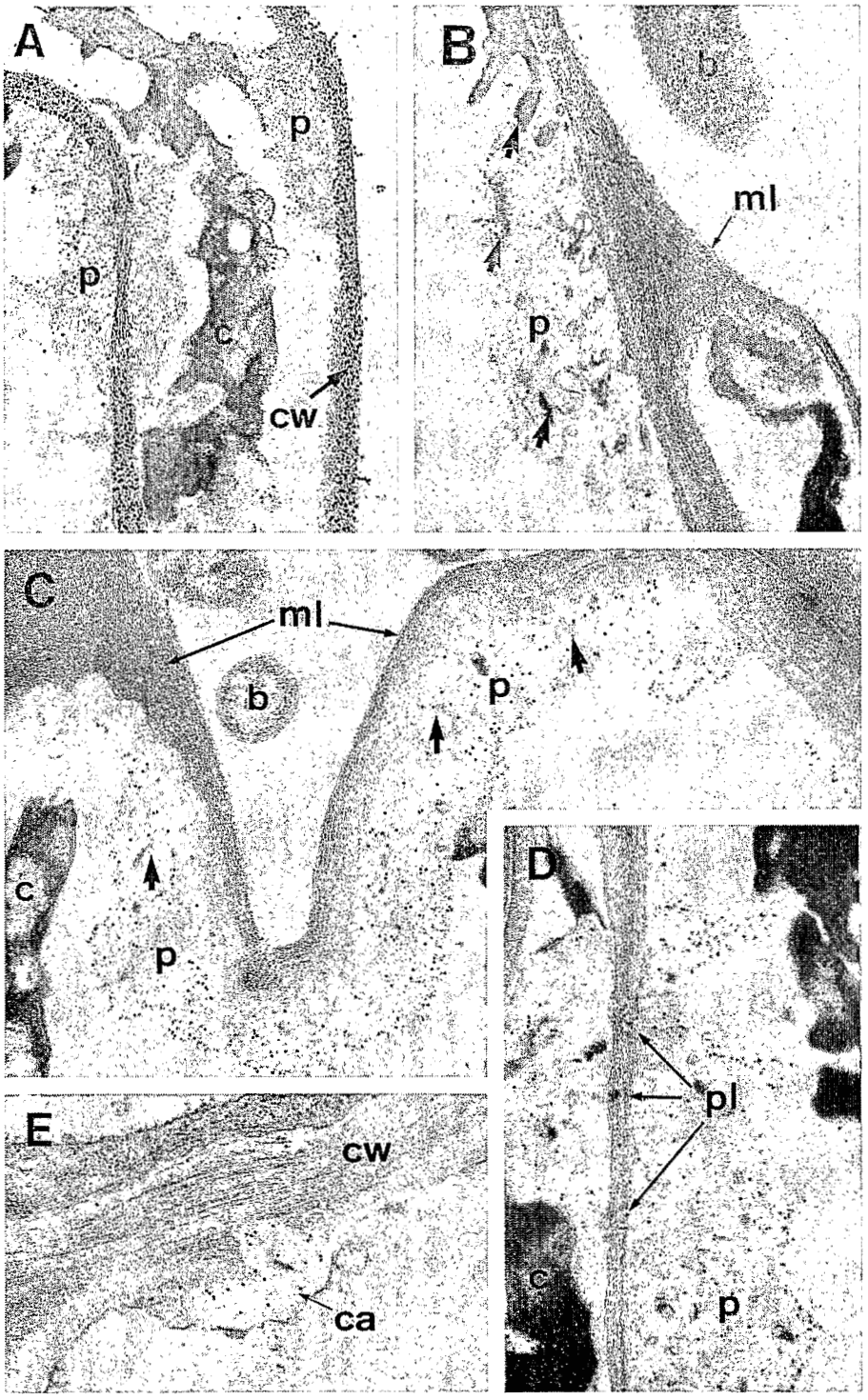

FIG. 7. Transmission electron micrographs of transverse sections in infected portions (A–D) or water-infiltrated areas (E) of cotyledons from the resistant cotton cultivar Reba B50. (A) Cytolocalization of β-1,4-D-glucans using an exoglucanase conjugated to colloidal gold. Gold particles are evenly distributed over walls of mesophyll cells (cv). No or few particles are seen over the paramural deposits (p). (c: coagulated cytoplasm; ×33000). (B) Immunogold localization of pectin epitopes after incubation of sections with the JIM 5 monoclonal antibody followed by goat anti-rat (GAT-10) secondary antibodies. Labelling is observed over the middle lamella (ml) between these mesophyll cells. No decoration is seen over the paramural deposit (p) that contains

TABLE 2
Multiplication of Xanthomonas campestris *pv.* malvacearum *in the susceptible and the resistant lines.*

Time (h)	log cfu $cm^{-2} \pm SD$	
	Susceptible	Resistant
0	7·02±0·13	6·24±0·05
2	6·91±0·03	6·62±0·06
6	7·07±0·02	6·74±0·25
24	8·20±0·15	8·07±0·01
48	9·43±0·22	8·9±0·05
72	10·1±0·28	9·86±0·2
120	7·98±0·34	10·99±0·18
168	6·82±0·19	10·42±0·22
216	6·66±0·22	10·2±0·3

Data shown are from a single representative experiment and are the means of three replicates for each line at each time.

vacuolar or cytoplasmic peroxidases [*43*, *47*, *53*]. A semi-quinoid form occurring after oxidation of a catechol nucleus potentiated the antimicrobial activity of several caffeic esters [*2*]. Also, ionically wall-bound peroxidases may be associated with the high level of phenolic esters incorporated into the cell wall of *Medicago* embryogenic culture [*34*]. In line with these observations, we suggest that peroxidase activity in infected cotton may be involved in flavonoid incorporation into cell wall polysaccharides in, or close to, the necrotic tissues. Indeed, peroxidase activity and flavonoid compounds were detected both in the cytoplasm and walls of mesophyll cells.

In conclusion, the ultrastructural and histochemical data from the present study support the concept that during the incompatible interaction between the cotton resistant line Reba B50 and *Xcm* race 18, flavonoid synthesis is activated in mesophyll cells close to infection sites. No increased staining for lignin, suberin, catechin and condensed tannins was seen. Flavonoids are produced within the cytoplasm and accumulated in cell walls and paramural papillae. We suggest that wall-bound peroxidases, the activity of which was histochemically detected before flavonoid accumulation, may play a role in the incorporation of these compounds in cell barriers. Associated with local deposition of callose and terpenoid synthesis that occurred later, flavonoid accumulation is an early defense response to *Xcm* in hypersensitive cotton cotyledons.

The authors wish to thank Dr R. Nicholson (Purdue University, West LaFayette), Dr D. Rumeau (CNRS-CEA, Cadarache), Dr D. Fernandez (ORSTOM, Montpellier)

electron-dense material (arrows) (×33000). (C–E) Immunogold localization of β-1,3-glucans after incubation of sections with polyclonal antibodies followed by goat anti-rabbit (GAR-15) secondary antibodies. (C, D) Labelling is present over the paramural material (p) deposited in mesophyll cells in the necrotic area (C, D). In D, the labelled papilla is located close to a plasmodesmatal area. No or very few gold particles are seen over the middle lamella (ml), the remaining cytoplasm (c) and the bacteria (b). Note the presence of electron-dense compounds within the papilla (arrows). (C: ×28000); D: ×27000). (E) In the phloem of the non-infected leaf portion, gold particles are distributed over the electron-lucent material deposited close to plasmodesmata of sieve tubes (ca: callose; cw: cell wall) (×33000).

Reproduced here at 80%.

and Dr F. Daayf (Université Lavel, Québec) for their helpful comments during the preparation of the manuscript.

REFERENCES

1. **Al-Mousawi AH, Richardson PE, Essenberg M, Johnson WM.** 1982. Ultrastructural studies of a compatible interaction between *Xanthomonas campestris* pv. *malvacearum* and Cotton. *Phytopathology* **72**: 1222–1230.
2. **Andary C.** 1993. Caffeic acid glycoside esters and pharmacology. In: Scolbert A, ed. *Polyphenolic phenomena*. Paris: INRA éditions, 237–245.
3. **Benhamou N, Lafontaire PJ, Nicole M.** 1994. Seed treatment with chitosan induces systemic resistance to *fusarium* crown, and root rot in tomato plants. *Phytopathology* **45**: 1432–1444.
4. **Benhamou N, Chamberland H, Ouellette GB, Pauzé FJ.** 1987. Ultrastructural localization of β-1,4-glucans in two pathogenic fungi and their host tissues by means of an exoglucanase-gold complex. *Canadian Journal of Microbiology* **33**: 405–417.
5. **Bestwick CS, Bennett MH, Mansfield J.** 1995. *hrp* mutant of *Pseudomonas syringae* pv. *phaseolicola* induces cell wall alteration but not membrane damage leading to the HR in lettuce *Lactuca sativa*. *Plant Physiology* **108**: 503–516.
6. **Boher B, Kpémoua K, Nicole M, Luisetti J, Geiger JP.** 1995. Ultrastructure of interactions between cassava and *Xanthomonas campestris* pv. *manihotis*. Cytochemistry of cellulose and pectin degradation in a susceptible cultivar. *Phytopathology* **85**: 777–788.
7. **Boher B, Brown I, Nicole M, Kpémoua K, Bonas U, Geiger JP, Mansfield J.** 1996. Histology and cytochemistry of interactions between plants and *Xanthomonas*. In: Nicole N, Gianinazi-Pearson V, eds. *Histology, Ultrastructure and Molecular Cytology of Plant-Microorganism Interactions*. Dordrecht: Kluwer Academic publishers, 193–210.
8. **Brinkerhoff LA. 1970.** Variation in *Xanthomonas malvacearum* and its relation to control. *Annual Review of Phytopathology* **8**: 85–110.
9. **Brown I, Mansfield J, Bonas U. 1996.** *hrp* genes in *Xanthomonas campestris* pv. *vesicatoria* determine ability to suppress papilla deposition in pepper mesophyls cells. *Molecular Plant-Microbe Interactions* **8**: 825–836.
10. **Cason ET Jr, Richardson PE, Essenberg MK, Brinkerhoff LA, Johnson WM, Venere RJ.** 1978. Ultrastructural cell wall alterations in immune cotton leaves inoculated with *Xanthomonas malvacearum*. *Phytopathology* **68**: 1015–1121.
11. **Daayf F, Nicole M, Boher B, Pando A, Geiger JP.** 1996. Early defense reactions of cotton roots to *Verticillium dahliae*. *European Journal of Plant Pathology*, (in press).
12. **Dai GH, Andary C, Mondolot-Cosson L, Boubals D.** 1995. Histochemical response of leaves of *in vitro* plantlets of *Vitis* spp. to infection with *Plasmopara viticola*. *Phytopathology* **85**: 149–154.
13. **Dai GH, Andary C, Mondolot-Cosson L, Boubals D.** 1995. Histochemical studies on the interaction between three species of grapevine, *Vitis vinifera*, *V. rupestris* and *V. rotundifolia* and the downy mildew fungus, *Plasmopara viticola*. *Physiological and Molecular Plant Pathology* **46**: 177–188.
14. **Dai GH, Andary C, Mondolot-Cosson L, Boubals D.** 1995. Involvement of phenolic compounds in the resistance of grapevine callus to downy mildew (*Plasmopara viticola*). *European Journal of Plant Pathology* **101**: 541–547.
15. **Davis EM, Tsuji J, Davis GD, Pierce ML, Essenberg M.** 1996. Purification of (+)-delta-cadinene synthase, a sesquiterpene cyclase from bacteria-inoculated cotton foliar tissue. *Phytochemistry* **41**: 1047–1055.
16. **De Feyter R, Yang Y, Gabriel DW.** 1993. Gene-for-genes interactions between cotton R genes and *Xanthomonas campestris* pv. *malvacearum*. *Molecular Plant-Microbe Interactions* **6**: 225–237.
17. **Deysson G.** 1954. *Eléments d'anatomie des plantes vasculaires*. Sedes, Paris.
18. **Essenberg M, Pierce M.** 1994. Sesquiterpenoid phytoalexins synthesized in cotton leaves and cotyledons during the hypersensitive response to *Xanthomonas campestris* pv. *malvacearum*. In: Daniel M, Purkayastha RP, eds. *Handbook of Phytoalexin Metabolism and Action*. New York, Basel, Hong Kong: Marcel Dekker, Inc, 183–198.
19. **Essenberg M, Grover PB Jr, Cover EC.** 1990. Accumulation of antibacterial sesquiterpenoids in bacterially inoculated *Gossypium* leaves and cotyledons. *Phytochemistry* **29**: 3107–3113.
20. **Essenberg M, Pierce M, Cover EC, Hamilton B, Richardson PE, Scholes VE.** 1992. A method for determining phytoalexin concentration in fluorescent, hypersensitively necrotic cells in cotton leaves. *Physiological and Molecular Plant Pathology* **41**: 101–109.

21. **Essenberg M, Pierce M, Hamilton B, Cover EC, Scholes VE, Richardson PE.** 1992. Development of fluorescent, hypersensitively necrotic cells containing phytoalexins adjacent to colonies of *Xanthomonas campestris* pv. *malvacearum* in cotton leaves. *Physiological and Molecular Plant Pathology* **41**: 85–99.
22. **Essenberg M, Doherty M, Hamilton BK, Henning VT, Cover EC, Mcfaul SJ, Johnson WM.** 1982. Identification and effects on *Xanthomonas campestris* pv. *malvacearum* of two phytoalexins from leaves and cotyledons of resistant cotton. *Phytopathology* **72**: 1349–1356.
23. **Follin JC.** 1983. Races de *Xanthomonas campestris* pv. *malvacearum* Smith. Dye en Afrique de l'Ouest et en Afrique Centrale. *Coton et Fibres tropicales* **38**: 274–279.
24. **Gahan PB.** 1984. *Plant Histochemistry and Cytochemistry.* London: Academic Press Ltd.
25. **Gardner RO.** 1975. Vanillin-hydrochloric acid as a histochemical test for tannins. *Stain Technology* **50**: 315–317.
26. **Goodman RN, Novacky AJ.** 1994. *The Hypersensitive Reaction in Plants to Pathogens.* St Paul: APS Press.
27. **Gorski PM, Vickstrom TE, Pierce ML, Essenberg M.** 1992. A C-13-pulse-labeling study of phytoalexin biosynthesis in hypersensitively responding cotton cotyledons. *Physiological and Molecular Plant Pathology* **47**: 339–355.
28. **Guo A, Reimers PJ, Leach JE.** 1993. Effect of light on incompatible interaction between *Xanthomonas oryzae* pv. *oryzae* and rice. *Physiological and Molecular Plant Pathology* **42**: 413–425.
29. **Gutmann M, Feucht W.** 1991. A new method for selective localization of flavan-3-ols in plant tissues involving glycolmethacrylate embedding and microwave irridation. *Histochemistry* **96**: 83–86.
30. **Hariri B, Sallé G, Andary C.** 1991. Involvement of flavonoids in the resistance of two poplar cultivars to mistletoe *Viscum album* L. *Protoplasma* **162**: 20–26.
31. **Hillocks RJ.** 1992. *Cotton Disease.* CAB International. Melksham: Redwood Press.
32. **Holliday MJ, Keen NT.** 1982. The role of phytoalexins in resistance of soybean leaves to bacteria: effect of glycophosphate on glyceollin accumulation. *Phytopathology* **72**: 1470–1474.
33. **Holton TA, Cornish EC.** 1995. Genetics and biochemistry of anthocyanin biosynthesis. *The Plant Cell* **7**: 1071–1083.
34. **Hrubcova M, Cvikrova M, Eder J.** 1994. Peroxidase activities and contents of phenolic acids in embryogenic and nonembryogenic alfalfa cells suspension cultures. *Biologia Plantarum* **36**: 175–182.
35. **Imberty A, Goldberg R, Catesson AM.** 1984. Tetramethylbenzidine and p-phenylenediamine-pyrocatechol for peroxidase histochemistry and biochemistry: two new, non-carcinogenic chromogens for investigating lignification process. *Plant Science Letter* **35**: 103–108.
36. **Jalali BL, Singh G, Grover RK.** 1976. Role of phenolics in bacterial blight resistance in Cotton. *Acta Phytopathologica Academia Sciencia Hungaria* **11**: 81–83.
37. **Jensen WA.** 1962. *Botanical Histochemistry.* San Francisco: Freeman.
38. **Knox JP, Linstead PJ, King J, Cooper C, Roberts K.** 1990. Pectin esterification is spatially regulated both within cell walls and between developing tissues of root apices. *Planta* **181**: 512–521.
39. **Kpémoua K, Boher B, Nicole M, Calatayud P, Geiger JP.** 1996. Cytochemistry of defense responses in cassava infected by *Xanthomonas campestris* pv. *manihotis. Canadian Journal of Microbiology*, **42**.
40. **Kobayashi A, Koguchi Y, Kanzaki H, Kajiyama S, Kawazu K.** 1994. A new type of antimicrobial phenolics produced by plant peroxidases and its possible role in the chemical defense systems against plant pathogens. *Zeitschrift für Naturforschung* **49c**: 411–414.
41. **Mace ME, Bell AA, Stipanovic RD.** 1974. Histochemistry and isolation of gossypol and related terpenoids in roots of cotton seedlings. *Phytopathology* **64**: 1297–1302.
42. **Maehly AC, Chance B.** 1954. The assay of catalase and peroxidase. In: Glick D, ed. *Methods of Biochemical Analysis.* New York: Interscience Publ. Co, 357.
43. **Morales M, Pedren MA, Barcelo AR, Calderon AA.** 1993. Oxidation of flavonol and flavonol glycosides by a hypodermal peroxidase isozyme from Gamay Rouge grape *Vitis vinifera.* berries. *Journal of Scientific Food Agriculture* **62**: 385–391.
44. **Morgham AT, Richardson PE, Essenberg M, Covers EC.** 1988. Effects of continuous dark upon ultrastructure, bacterial population and accumulation of phytoalexins during interactions between *Xanthomonas campestris* pv. *malvacearum* and bacterial blight susceptible and resistant cotton. *Physiological and Molecular Plant Pathology* **32**: 141–162.
45. **Neu R.** 1956. A new reagent for differentiating and determining flavones on paper chromatograms. *Naturwissenschaften* **43**: 82.
46. **Northcote DH, Davey R, Lay J.** 1989. Use of antisera to localize callose, xylan, and arabinogalactan in the cell-plate, primary and secondary walls of plant cells. *Planta* **178**: 353–366.
47. **Patzlaff M, Barz W.** 1978. Peroxidatic degradation of flavanones. *Zeitschrift für Naturforschung* **33c**: 675–684.
48. **Peng M, Kuc J.** 1992. Peroxidase-generated hydrogen peroxide as source of antifungal activity in vitro and on tobacco leaf disks. *Phytopathology* **82**: 696–699.

49. **Pierce M, Essenberg M.** 1987. Localization of phytoalexins in fluorescent mesophyll cells isolated from bacterial blight-infected cotton cotyledons are separated from other cells by fluorescence-activated cell sorting. *Physiological and Molecular Plant Pathology* **31**: 273–290.
50. **Reimers PJ, Leach JE.** 1991. Race-specific resistance to *Xanthomonas oryzae* pv. *oryzae* conferred by bacterial blight resistance gene Xa-10 in rice *Oryza sativa* involves accumulation of a lignin-like substance in host tissues. *Physiological and Molecular Plant Pathology* **38**: 39–55.
51. **Reimers PJ, Ringl C, Dudler R.** 1992. Complementary DNA cloning and sequence analysis of a pathogen-induced peroxidase from rice. *Plant Physiology* **100**: 1611–1612.
52. **Snyder BA, Nicholson RL.** 1990. Synthesis of phytoalexins in sorghum as a site-specific response to fungal ingress. *Science* **248**: 1585–1588.
53. **Takahama U.** 1988. Oxidation of flavonols by hydrogen peroxide in epidermal and guard cells of *Vicia faba* L. *Plant Cell Physiology* **29**: 433–438.
54. **Taylor JA, West DW.** 1980. The use of Evan's blue stain to test the survival of plant cells after exposure to high salt and high osmotic pressure. *Journal of Experimental Botany* **31**: 571–576.
55. **Venere RJ.** 1980. Role of peroxidase in cotton resistant to bacterial blight. *Plant Science Letters* **20**: 47–56.
56. **Wyman JG, VanEtten HD.** 1978. Antibacterial activity of selected isoflavonoids. *Phytopathology* **68**: 583–589.